DOI: 10.1002/ejic.200600938

Bonding Properties Related with Chiral Discrimination in Dinuclear Metal Complexes of Group 10

Oscar Picazo,[a] Ibon Alkorta,*[a] José Elguero,[a] Markku R. Sundberg,*[b] and Jaana Valo[b]

Keywords: Ab initio calculations / Coordination chemistry / Chiral discrimination / Bonding properties / *trans* influence

A series of neutral dinuclear homo- and heterochiral complexes formed by hydrazine (a molecule with axial chirality), a metal atom of group 10 (Ni, Pd, Pt), and halogen atoms (F, Cl, Br, I) was studied by computational methods including density functional theory. In the optimized structures the heterochiral complexes were always found to be energetically favored. The chiral discrimination depends on the contributions coming from the metal atoms and the halogen anions attached to them. Moreover, the relative energies of the optimized complexes are correlated with the electronegativity of the metals and the halogens as well as with the relative distances of the bond critical points in the metal–nitrogen bonds. Also the smaller deviation of the ligand–metal–ligand angles from the ideal value of 90° corresponds to the heterochiral complexes. An analysis of the bonding properties reveals a complex mechanism for the behavior of the electron lone pairs of the nitrogen and halogen atoms. The electronic properties of the optimized complexes were studied by NBO (Natural Bond Orbital) and QTAIM (Quantum Theory of Atoms in Molecules) methods. An NBO analysis of the energy differences between the stabilizing energies related to the interactions between an electron lone pair of the coordinated nitrogen atom and the opposite M–X antibonding orbital explain the differences of the total energies between the diastereomeric heterochiral and homochiral complexes. The stabilizing energies have systematically more negative values in the heterochiral complexes; this can be interpreteted as a measure of the *trans* influence. Small energy values related to the *cis* influence were found mainly in the nickel complexes. The M–N bonds in the heterochiral complexes are more polar with a higher bond order than that in the homochiral ones, as shown by QTAIM methods.

Introduction

In order to understand the chemical properties of a compound it is necessary to know not only the structure, but also the electronic properties and their mutual relationship. Computational methods offer a means to elucidate both aspects. We employ here DFT (Density Functional Theory) calculations to evaluate the structural and electronic characteristics of dinuclear hydrazine complexes formed by group 10 metals displaying chiral discrimination. To understand the correlations between structural and electronic properties in metal complexes it is necessary to consider concepts related with the deformations in the coordination polyhedra.

Chiral recognition is an important concept in many chemical processes, for which nonlinear effects in asymmetric synthesis and stereoselective reactions are some examples.[1] Peroxides and hydrazine present axial chirality with low racemization barriers.[2,3] The presence of different chiral molecules of hydrazine has been used to explain the experimental results of clusters in the gas phase.[4] A topic that has received only a limited experimental interest so far is chiral biodiscrimination based upon axial chirality. As an example, mutations at the putative distal site of cytochrome P450 have been shown to be dependent on axial chirality.[5]

The factors leading to chiral discrimination have been computationally studied only a few times in metal complexes or related systems. The effect of fluoro substitution on the chiral discrimination has been discussed in bis(diphenylborate)s and isoelectronic structures.[6] In addition, 1:1 and 2:1 complexes of chiral bis(5*H*-pyrrole)s and bis(oxazoline)s with the lithium cation have been shown to favor the heterochiral complexes, except for the *tert*-butyl derivatives.[7]

The *trans* influence, also called structural *trans* effect, is one of the key concepts in understanding the structure-bonding relation in metal complexes.[8] The concept involves the idea that a bond *trans* to a donor atom should be longer and weaker than that in a *cis* position. The influence has been evaluated by using statistical methods applied

[a] Instituto de Química Médica (C.S.I.C.)
Juan de la Cierva 3, 28006 Madrid, Spain
Fax: +34-91-564-4853
E-mail: ibon@iqm.csic.es
[b] Laboratory of Inorganic Chemistry, Department of Chemistry, University of Helsinki
P. O. Box 55 (A. I. Virtasen aukio 1), 00014 Helsinki, Finland
Fax: +958-9-19150198
E-mail: markku.sundberg@helsinki.fi
Supporting information for this article is available on the WWW under http://www.eurjic.org or from the author.

to existing structural data[9] by using a theoretical approach[10] as well as computational methods.[11–14] Related to the *trans* influence there is also an analogous *cis* influence. Their mutual relative magnitude is obviously dependent on the electron configuration of a central metal atom.[9]

In an earlier study on (phosphane)molybdenum complexes[12] the amount of *trans* influence was found to be dependent on the angular distortion on the coordination sphere and consequently on the overlap between the metal d orbital and the phosphane σ* orbitals. The importance of the electronic occupation on antibonding orbitals was established earlier by Burdett and Albright.[11] A correlation between the *trans* influence and bond order values was found in *cis*-dichloridobis(triphenylstibane)platinum.[15] Interestingly, the *trans* influence has been shown to have an important role in creating new Pd^{II} complexes with nonlinear optical properties.[16]

In general, the geometry around a central metal atom in the complexes is dependent on the electronic properties. Among the concepts to be taken into account are the Jahn–Teller effect, the pseudo-Jahn–Teller effect, and Bent's rule. In our case, only the last concept might be relevant, since the planar complexes of the group 10 metals do not have an electronic configuration involving unpaired electrons.

There have been discussions about the applicability of Bent's rule on transition metal complexes. When applied to the main group elements, Bent's rule states that the more electronegative substituents are related with more central-atom p-orbital character resulting in smaller angles, whereas the less electronegative subsituents obtain more s-orbital character and consequently wider angles.[17] However, the bonding in transition metal complexes involves not only s- but essentially also d-orbitals, and thus the situation is essentially different.[18] Although Bent's rule has been reformulated by Frenking et al.,[19] it seems that Bent's rule will be of limited use for transition metal complexes.[20]

The studied complexes are related to *cis*-platinum and the newly described asymmetric *trans*-platinum(II) complexes, which have shown anticancer activity.[21] In addition, hydrazine in the presence of manganese and copper ions has been evaluated for site-specific DNA damage.[22] On the other hand, both platinum and palladium have the propensity to form dinuclear complexes.[23] The idea surrounding the synthesis of hydrazine-bridged dinuclear platinum complexes is that they should be able to crosslink two adjacent bases of DNA without bending the double helix.[24] Some dinuclear platinum complexes containing N-mediated bridges have been shown to be cytotoxic.[25,26] However, none of these contained two similar bridges. In our preliminary communication we have shown, by computational methods, how the doubly hydrazine-bridged dinuclear complexes formed by halogens and group 10 metal cations display axial discrimination.[27]

In this paper we study the electronic properties of the doubly bridged hydrazine complexes in more detail by using computational methods. The basic question related to our work is whether electronic properties could explain the differences in the energies between the diastereomer homochiral and heterochiral complexes. Special emphasis was placed on the importance of the electron lone pairs of the coordinated atoms and their role in complex formation.

Results and Discussion

1. Energy

The complexes under study are dinuclear with two neutral hydrazine molecules acting as bridges. The planar coordination sphere around each metal atom of group 10 (Ni, Pd, Pt) is formed by two nitrogen atoms of two hydrazine molecules and two halogen atoms (F, Cl, Br, I). The axial chirality (noted as subscript a) of hydrazine results in two diastereomeric complexes, namely homochiral [(R_a/R_a) or (S_a/S_a)] and heterochiral [(R_a/S_a) or (S_a/R_a)] complexes. Hereafter, the notifications *RR* and *RS* will be used for the homochiral and heterochiral enantiomers, respectively.

The optimized geometry of the complexes presents D_2 and C_{2h} symmetry for all the homochiral and heterochiral cases, respectively. Typical structures are shown in Figure 1.

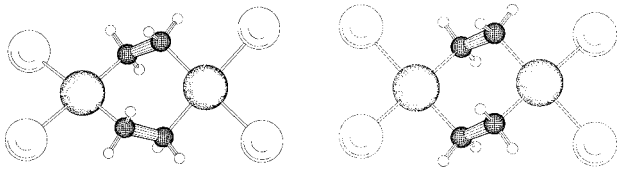

Figure 1. The *RS* (left) and *RR* (right) diasteromers of dinuclear metal complexes formed by hydrazine molecules and halogen atoms.

The energies for the optimized complexes at the B3LYP/LANL2DZ level of theory are shown in Table 1, as well as the relative energies, E_{rel}. The relative energy E_{rel} is defined as $E_{rel} = E_{RS} - E_{RR}$.

In all the hydrazine derivatives the heterochiral complexes are favored over the homochiral ones, with energy differences that range between 1.4 and 3.8 kcal/mol. As the size of the metal atom increases the differences also increase; the opposite takes place with the size of the halogen atoms, the largest differences are found for fluorine and the smallest for iodine for a given metal complex. Although the differences are relatively small, it is possible to see some trends by using statistical methods, as shown below.

A Free–Wilson correlation[28] [Equation (1)] was found between the presence/absence of each metal and halogen atom and the relative energy of the homo-/heterochiral pairs. The underlying hypothesis in a Free–Wilson approach is the independence of the effects of halogens and metals. In the equation the coefficient corresponding to the presence of Pt has been arbitrarily fixed to 1 and thus the rest of the contributions can be compared. The coefficient for each variable provides the energy contribution to the chiral selectivity in each pair using as a reference the homochiral system. It must be underlined that the Free–Wilson method gives no direct physicochemical interpretation.

Table 1. Total energy [hartree] and relative energy, E_{rel} [kcal/mol; 1 kcal/mol = 4.1868 kJ/mol], of the hydrazine complexes $[MX_2hy]_2$ (M = Ni, Pd, Pt; X = F, Cl, Br, I; hy = hydrazine) calculated at the B3LYP/LAN2DZ computational level. The compounds are identified by their MX_2 fragments.

Fragment	Chirality	Total energy	E_{rel}
NiF_2	*RR*	–961.965473	0
NiF_2	*RS*	–961.969945	–2.805
$NiCl_2$	*RR*	–622.399674	0
$NiCl_2$	*RS*	–622.402660	–1.876
$NiBr_2$	*RR*	–615.266813	0
$NiBr_2$	*RS*	–615.269359	–1.598
NiI_2	*RR*	–608.133750	0
NiI_2	*RS*	–608.135931	–1.368
PdF_2	*RR*	–876.761868	0
PdF_2	*RS*	–876.766906	–3.161
$PdCl_2$	*RR*	–537.238303	0
$PdCl_2$	*RS*	–537.241901	–2.258
$PdBr_2$	*RR*	–530.122256	0
$PdBr_2$	*RS*	–530.125219	–1.859
PdI_2	*RR*	–523.008274	0
PdI_2	*RS*	–523.010781	–1.575
PtF_2	*RR*	–861.614577	0
PtF_2	*RS*	–861.620643	–3.806
$PtCl_2$	*RR*	–522.079012	0
$PtCl_2$	*RS*	–522.083867	–3.047
$PtBr_2$	*RR*	–514.960402	0
$PtBr_2$	*RS*	–514.964730	–2.716
PtI_2	*RR*	–507.847389	0
PtI_2	*RS*	–507.851357	–2.491

$$E_{rel}\,[\text{kcal/mol}] = -4.89(\text{F}) - 4.03(\text{Cl}) - 3.69(\text{Br}) - 3.45(\text{I}) + 2.10(\text{Ni}) + 1.80(\text{Pd}) + 1.00(\text{Pt}) \quad (1)$$

The statistical r^2 value in Equation (1) is 0.996. The coefficients for the halogens are always negative and for the metals positive. Moreover, the absolute values of the weights for the halogen atoms are larger than those of the metal atoms. The smaller and more electronegative a counter anion is, the larger its negative weight will be. Such a clear relation between the coefficients of Equation (1) and the electronegativity values for the group 10 metal atoms does not exist.

The energy differences are also strongly correlated with the electronegativity values of the participating metals and halogens [Equation (2), where χ refers to the Pauling electronegativity values recalculated by Allred[29]].

$$E_{rel} = 4.13 - 1.11\chi\text{Hal} - 1.29\chi\text{Met} \quad (2)$$

The r^2 value for the correlation is 0.991. According to the original idea of Linus Pauling, electronegativity describes the electron-withdrawing capacity of an atom. It is clear that the electron-withdrawing capacity must be distance-dependent. Therefore, we may assume at this stage that the relative energies should correlate with the M–L bond lengths.

Both of the equations contain parameters that are isotropic. However, we may well assume that the energy differences should be because of the differences in bonding in the complexes. On the other hand, the bonds have a directionality, thus destroying the spherical symmetry. Therefore, the bonds and their properties should be examined.

The parameter connected with the deformation of spherical symmetry is the bond angle. Selected bond angles of the optimized complexes are gathered in Table 2 in which there are two additional parameters displayed. The first one, Σdef, gives the sum of the absolute values of the deformation of the angles from the ideal value of 90°. The second one, ΔΣdef, is the difference between the Σdef values between the heterochiral and homochiral complexes.

Table 2. Selected geometrical parameters of the hydrazine complexes optimized at the B3LYP/LANL2DZ level (bond lengths in Å, bond angles and dihedral angles in °).

Fragment	Chirality	X–M–X	N–M–N	X–M–N	Σdef	ΔΣdef
NiF_2	*RR*	99.47	99.36	80.63	28.60	
NiF_2	*RS*	99.14	98.23	81.26	26.11	–2.09
$NiCl_2$	*RR*	95.91	95.24	84.42	16.73	
$NiCl_2$	*RS*	96.32	93.41	85.01	14.72	–2.01
$NiBr_2$	*RR*	95.07	94.45	85.25	14.27	
$NiBr_2$	*RS*	95.06	92.45	86.12	11.39	–2.88
NiI_2	*RR*	94.30	93.61	86.22	11.69	
NiI_2	*RS*	94.25	91.33	87.08	8.50	–3.19
PdF_2	*RR*	101.6	103.6	77.42	37.8	
PdF_2	*RS*	101.7	102.8	77.73	35.8	–2.00
$PdCl_2$	*RR*	96.89	98.91	82.11	23.79	
$PdCl_2$	*RS*	96.99	97.33	82.82	21.50	–2.29
$PdBr_2$	*RR*	94.51	97.55	83.98	18.08	
$PdBr_2$	*RS*	94.77	95.87	84.66	15.98	–2.10
PdI_2	*RR*	92.49	95.85	85.83	12.41	
PdI_2	*RS*	93.00	93.94	86.50	10.44	–1.97
PtF_2	*RR*	101.1	103.9	77.54	37.5	
PtF_2	*RS*	101.2	102.9	77.91	36.2	–1.30
$PtCl_2$	*RR*	97.19	99.42	81.71	24.90	
$PtCl_2$	*RS*	97.34	97.71	82.47	22.58	–2.32
$PtBr_2$	*RR*	95.20	98.05	83.39	19.86	
$PtBr_2$	*RS*	95.55	96.11	84.17	17.49	–2.37
PtI_2	*RR*	93.60	96.13	85.14	14.59	
PtI_2	*RS*	94.17	93.96	85.92	12.11	–2.48

The ΔΣdef values are always negative (between –1.30 and –3.19°) meaning that the angles are closer to the ideal value of 90° for the heterochiral complexes. It is important to note that for the dications of the group 10 metals the empty d-orbital is the $d_{x^2-y^2}$. This orbital is used in the bond formation between a metal cation and the four ligand atoms. The plausible explanation for the relative stability of the heterochiral complexes is obviously the bigger overlap between the metal $d_{x^2-y^2}$-orbital and the electron lone pairs of the ligand atoms.

There are also some trends in the bond lengths. In the first two families (Ni and Pd) and for each pair of complexes the homochiral metal–halogen bond length is slightly shorter than the heterochiral one. Interestingly, the$M–N bond lengths tend to have larger values in the Pd and Pt complexes, whereas in the nickel complexes no trend can be seen. For all the metals studied here, the shortest M–X distances correspond to X = F, followed by Cl, Br and the longest ones are with I. This ordering is in accordance with the covalent radii of the halogen atoms and electronegativ-

ity scale of the X atoms. There is a correlation between the M–X and M–N bond lengths, which is shown in Figure 2.

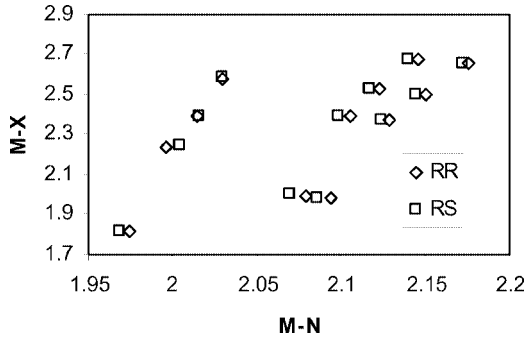

Figure 2. Scatter plot displaying the M–X vs. M–N bond length [Å]. There are six almost linear correlations to be seen, three of them corresponding to the *RS* and three to the *RR* families. From left to right the order is Ni, Pt, and Pd.

If the chirality is not taken into account, the analysis of the metal–halogen vs. metal–nitrogen bond lengths for the analogous complexes show good correlations for every metal family (r^2 values of 0.99 and higher).

It was not possible to establish any correlation with the relative energies and the M–L bond lengths, however, although this was expected based on the reasoning related to Equation (2). It is very important to note, however, that in the heterochiral complexes the M–N bond lengths have the propensity to be shorter than in their homochiral analogs. The opposite holds for the M–X bond lengths.

Owing to the different point groups, there are also differences in the torsional angles related to the hydrazine molecules. The homochiral and heterochiral complexes can be divided into two categories based on the torsional angles X–M–N–N and X–M–N–H_{eq}. Furthermore, there is a strong linear correlation between the torsional angles, as seen in Figure 3.

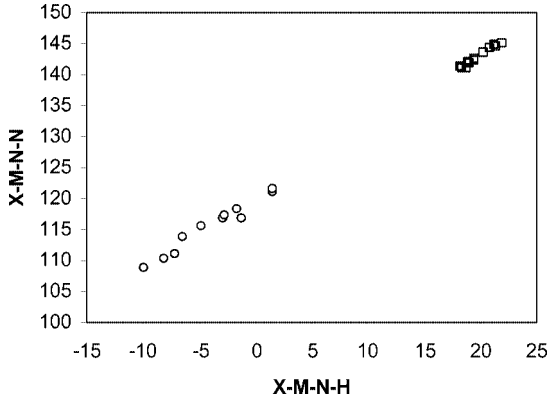

Figure 3. Scatter plot of the X–M–N–N and X–M–N–H torsional angles (in °). The hydrogen atom refers to that in the equatorial position. The spheres refer to the heterochiral complexes and the squares to the homochiral diasteromers.

2. Electronic Properties

To explain the differences in energy for the hetero- and homochiral complexes it is necessary to study the influence of the electron lone pairs of the coordinated atoms. To obtain qualitative numerical values to characterize the influence both QTAIM and NBO methods were employed. Since both N–M–N angles and M–N bond lengths are relatively strongly affected by the central metal atom and the halogen atoms, special emphasis was laid on the bonding properties of the M–N bonds.

2.1 Topological Analysis of Charge Density

In QTAIM theory a bond between two atoms is characterized by a line of maximum electron density (i.e. the bond path), which connects the two nuclei and intersects a zero-flux surface in the gradient field at a (3,–1) saddle point (i.e. the bond critical point). There are several descriptive parameters at the bond critical point that can be used to characterize the interaction between two atoms. These are the electron density $\rho(r)$ and its Laplacian $\nabla^2\rho(r)$. The Laplacian of the electronic charge density characterizes the two extreme conditions: either the charge density is locally concentrated [$\nabla^2\rho(r) < 0$] or it is locally depleted [$\nabla^2\rho(r) > 0$]. In the former case the bond has a covalent character, whereas in the latter case the interaction can be understood in terms of a closed-shell interaction. The eigenvalues λ_1, λ_2, and λ_3 of the Hessian describe the curvature of the gradient field at the bond critical point. The ellipticity ε of a bond is defined as $\varepsilon = \lambda_1/\lambda_2 - 1$. Furthermore, the local electronic energy density $E_d(r)$ is the sum of the local kinetic and potential energy density, $E_d(r) = G(r) + V(r)$. A detailed discussion of the parameters can be found in ref.[27] Descriptive QTAIM parameters related to the bond critical points for the M–N bonds are given in Table 3.

The M–N bonds are all polar bonds, as is the case usually with the coordinate bonds.[31] This is seen in the positive Laplacian [$= \nabla^2\rho(r)$] values, which indicate charge depletion in the bond critical points. The charge depletion is clearly seen in Figure 4 where the negative Laplacian contour plot is given for the heterochiral $[NiF_2(hydrazine)]_2$ compound.

The ratio $|\lambda_1|/\lambda_3$, which is expected to be smaller than 1 in ionic bonds,[30a] shows very small values. As will be shown in the discussion related with the NBO results the coordinated nitrogen atoms carry a significant negative charge. Accordingly, the bonds also have a significant ionic nature. The potential electronic energy density dominates the kinetic electronic energy density at the bond critical points, and thus all $E_d(r)$ values are negative, thus indicating sharing of charge.[30a]

There is also an interesting difference seen in the coordination of fluorine and nitrogen in Figure 4. Both nitrogen atoms have an electron lone pair pointing approximately towards the central nickel atom, whereas the fluorine atoms have an almost isotropic distribution of the Laplacian of the charge density. This phenomenon will be discussed later on in more detail in connection with the NBO analysis.

It has been shown by Matta and Hernandez-Trujillo that there is a linear correlation between bond order and ellipticity.[32] As seen in Table 3, the ellipticity values always have larger values for the M–N bonds in the heterochiral

Table 3. Descriptive parameters for the bond critical bonds for the M–N bonds in the $[MX_2hy]_2$ complexes. The distance D [a.u.] is the distance of the bond critical point from the metal atom in an M–N bond.

Fragment	Chirality	D	$\rho(r)$ [e/ao3]	$\nabla^2\rho(r)$ [e/ao5]	λ_1	λ_2	λ_3	ε	$\lvert\lambda_1\rvert/\lambda_3$	$E_d(r)$ [a.u.]
NiF_2	*RR*	1.938	0.091	0.482	–0.109	–0.102	0.693	0.064	0.1573	–0.0188
NiF_2	*RS*	1.932	0.092	0.487	–0.112	–0.104	0.702	0.081	0.1595	–0.0199
$NiCl_2$	*RR*	1.987	0.081	0.439	–0.095	–0.090	0.624	0.054	0.1522	–0.0123
$NiCl_2$	*RS*	1.986	0.082	0.441	–0.098	–0.091	0.630	0.072	0.1556	–0.0129
$NiBr_2$	*RR*	1.995	0.079	0.435	–0.093	–0.088	0.615	0.053	0.1512	–0.0112
$NiBr_2$	*RS*	1.997	0.080	0.434	–0.094	–0.088	0.617	0.070	0.1524	–0.0115
NiI_2	*RR*	2.010	0.077	0.426	–0.089	–0.085	0.600	0.052	0.1483	–0.0096
NiI_2	*RS*	2.012	0.078	0.426	–0.091	–0.085	0.602	0.070	0.1512	–0.0100
PdF_2	*RR*	1.953	0.092	0.388	–0.093	–0.091	0.572	0.028	0.1626	–0.0238
PdF_2	*RS*	1.944	0.094	0.395	–0.096	–0.093	0.583	0.035	0.1647	–0.0247
$PdCl_2$	*RR*	1.982	0.087	0.351	–0.087	–0.082	0.519	0.067	0.1676	–0.0227
$PdCl_2$	*RS*	1.978	0.088	0.355	–0.089	–0.082	0.526	0.082	0.1692	–0.0232
$PdBr_2$	*RR*	2.000	0.083	0.336	–0.083	–0.078	0.497	0.069	0.1670	–0.0216
$PdBr_2$	*RS*	1.997	0.084	0.340	–0.085	–0.078	0.503	0.082	0.1690	–0.0220
PdI_2	*RR*	2.025	0.079	0.317	–0.078	–0.073	0.469	0.069	0.1663	–0.0201
PdI_2	*RS*	2.022	0.080	0.321	–0.080	–0.074	0.475	0.082	0.1684	–0.0205
PtF_2	*RR*	1.913	0.104	0.433	–0.097	–0.094	0.624	0.029	0.1554	–0.0257
PtF_2	*RS*	1.902	0.106	0.443	–0.099	–0.097	0.639	0.012	0.1549	–0.0268
$PtCl_2$	*RR*	1.932	0.099	0.403	–0.093	–0.087	0.582	0.067	0.1598	–0.0248
$PtCl_2$	*RS*	1.926	0.101	0.410	–0.094	–0.087	0.592	0.081	0.1588	–0.0255
$PtBr_2$	*RR*	1.947	0.096	0.389	–0.089	–0.083	0.562	0.078	0.1584	–0.0237
$PtBr_2$	*RS*	1.942	0.098	0.396	–0.091	–0.084	0.570	0.090	0.1596	–0.0243
PtI_2	*RR*	1.968	0.092	0.371	–0.085	–0.078	0.535	0.085	0.1589	–0.0222
PtI_2	*RS*	1.962	0.093	0.377	–0.087	–0.079	0.543	0.094	0.1602	–0.0228

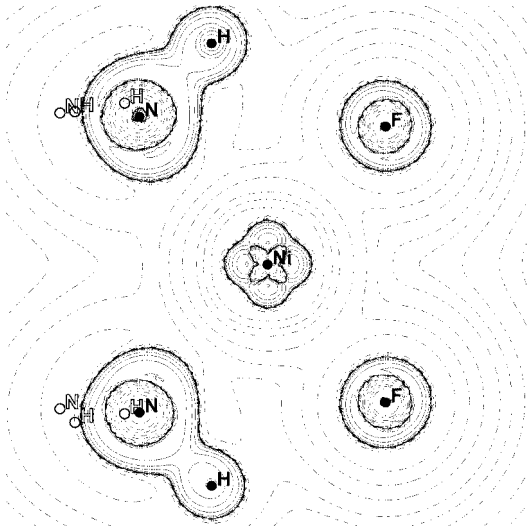

Figure 4. Laplacian contour map for *RS*-$[NiF_2(hydrazine)]_2$ (solid black line refers to positive values and the dotted ones to negative values of the Laplacian).

complexes, thus indicating a higher bond order in these bonds.

The only significant correlation to explain the relative energy E_{rel} with the parameters at the bond critical points was found with the relative distance D_{rel} of a bond critical point from a metal atom ($D_{rel} = D_{RR} - D_{RS}$) in the M–N bonds. The equation of the fitted model is Equation (3).

$$E_{rel} = -2.474 - 2374D_{rel} \quad (3)$$

Since the P value in the ANOVA (Analysis of Variance)[33] result is less than 0.05, there is a statistically significant relationship between E_{rel} and D_{rel} at the 95% confidence level. The r^2 statistic indicates that the model as fitted explains 89.3% of the variability in E_{rel}. The correlation coefficient equals –0.945, indicating a relatively strong relationship between the variables.

The differences between the positions of the bond critical points are thus correlated with the energy differences. The longer the distance of the bcp from a metal atom in an *RR* complex is with regard to the point in an *RS* analog, the more favored the *RS* complex will be in terms of energy. This is in accordance with the finding that the bond order is higher in the *RS* diastereomers.

2.2 NBO Analysis

To obtain a wider insight into the influence of the halogen ions on the M–N bonds and especially on the relative stabilities of the diastereomers we carried out additional analyses employing NBO methods.

There were no differences in the electronic configurations for the metals between different diastereomers. (The hybridization of the metals varied depending on the counter anion and metal species itself.) Thus, we may say that Bent's rule does not seem to play any significant role in explaining chiral discrimination. NBO charges for the metal, nitrogen, and halogen atoms are shown in Table 4.

The metal atom charges tend to have larger values in the heterochiral complexes than in their homochiral diastereomers. This tendency increases concomitantly with increasing Z. The highest absolute values are found for the nickel complexes and the lowest ones for the platinum complexes. The range of the charges goes from 0.3210 to 0.9889. The range for the halogen atom charges is also quite wide, from –0.3254 to –0.6567. The charge is always more negative in a heterochiral complex. The charges of the nitrogen

Table 4. NBO charges for the metal, nitrogen, and halogen atoms in the $[MX_2(hydrazine)]_2$ complexes.

Fragment	Chirality	M charge	N charge	X charge
NiF_2	*RR*	0.9887	–0.7219	–0.6539
NiF_2	*RS*	0.9889	–0.7187	–0.6567
$NiCl_2$	*RR*	0.7603	–0.7299	–0.5254
$NiCl_2$	*RS*	0.7614	–0.7202	–0.5308
$NiBr_2$	*RR*	0.6967	–0.7376	–0.4814
$NiBr_2$	*RS*	0.6977	–0.7267	–0.4877
NiI_2	*RR*	0.6257	–0.7487	–0.4297
NiI_2	*RS*	0.6260	–0.7365	–0.4365
PdF_2	*RR*	0.8749	–0.6943	–0.6271
PdF_2	*RS*	0.8786	–0.6930	–0.6314
$PdCl_2$	*RR*	0.6238	–0.7034	–0.4837
$PdCl_2$	*RS*	0.6274	–0.6977	–0.4888
$PdBr_2$	*RR*	0.5338	–0.7109	–0.4250
$PdBr_2$	*RS*	0.5370	–0.7047	–0.4307
PdI_2	*RR*	0.4259	–0.7205	–0.3531
PdI_2	*RS*	0.4282	–0.7140	–0.3596
PtF_2	*RR*	0.8651	–0.6921	–0.6321
PtF_2	*RS*	0.8744	–0.6931	–0.6359
$PtCl_2$	*RR*	0.5686	–0.6964	–0.4759
$PtCl_2$	*RS*	0.5756	–0.6930	–0.4803
$PtBr_2$	*RR*	0.4578	–0.7027	–0.4097
$PtBr_2$	*RS*	0.4637	–0.6983	–0.4148
PtI_2	*RR*	0.3210	–0.7116	–0.3254
PtI_2	*RS*	0.3254	–0.7064	–0.3313

Table 5. The main components (>1%) of the electron lone pairs of the nitrogen atoms. Percentage values are given.

Fragment	Chirality	N [%]	M [%]	X [%]
NiF_2	*RR*	88.463	8.688	1.704
NiF_2	*RS*	88.183	9.021	1.740
$NiCl_2$	*RR*	88.774	8.059	2.329
$NiCl_2$	*RS*	88.520	8.263	2.380
$NiBr_2$	*RR*	89.280	7.462	2.446
$NiBr_2$	*RS*	89.040	7.635	2.504
NiI_2	*RR*	89.999	6.715	2.489
NiI_2	*RS*	89.807	6.827	2.546
PdF_2	*RR*	87.090	9.604	2.228
PdF_2	*RS*	86.663	10.020	2.261
$PdCl_2$	*RR*	86.065	9.522	3.525
$PdCl_2$	*RS*	85.789	9.775	3.576
$PdBr_2$	*RR*	88.315	7.469	3.186
$PdBr_2$	*RS*	88.059	7.663	3.246
PdI_2	*RR*	89.252	6.464	3.282
PdI_2	*RS*	89.019	6.619	3.349
PtF_2	*RR*	86.127	10.569	2.439
PtF_2	*RS*	85.779	10.938	2.469
$PtCl_2$	*RR*	86.065	9.522	3.525
$PtCl_2$	*RS*	85.789	9.775	3.576
$PtBr_2$	*RR*	86.576	8.691	3.857
$PtBr_2$	*RS*	86.315	8.915	3.916
PtI_2	*RR*	87.322	7.679	4.147
PtI_2	*RS*	87.068	7.864	4.226

atoms vary considerably less, the range being from –0.6921 to –0.7487. Again there is a difference between the heterochiral and homochiral complexes; in the former ones the halogen charges are more negative than in the latter ones. This means that the M–X bonds in the heterochiral complexes have more ionic character than in the homochiral diastereomers.

To study the M–N bonds in more detail, an NLMO analysis was carried out. (A full description of the electron lone pair compositions is given as Supporting Information.) There was a profound difference between the halogen and nitrogen atoms. The nitrogen atoms clearly showed the expected hybridization, but the halogen atoms did not. In the halogen atoms the electron lone pair participating in the coordination to the metal atom always had a clear p-orbital character. The main components of the nitrogen lone pairs are given in Table 5.

According to the results, the electron lone pair of nitrogen in terms of the NLMO consists only partly of the localized electron lone pair of nitrogen but also of the halogen *trans* to the nitrogen and the metal atom. The electron lone pair is systematically more delocalized in the heterochiral complexes. The interpretation of the delocalization can be expressed by two different mechanisms. In the case of the metals, the delocalization can be interpreted simply by covalency of a metal–nitrogen bond, which is higher in the M–N bonds of the heterochiral complexes. As for the halogens, their contribution is opposite to the mechanism of the *trans* influence, where the electron transfer should take place to an antibonding orbital. In our case the stabilizing energy found for this contribution is less than 0.1 kcal/mol. Instead, the contribution can be explained in terms of 3c–4e bonding. The NBO analyses were not able to directly find the M–N or X–M–N bonds because of the pronounced polarity of these bonds, and an illustration (Figure 5) for the formal M–N bonding orbital produced by NBOView corroborates this assumption. Furthermore, the interactions are found in the NLMO listings.

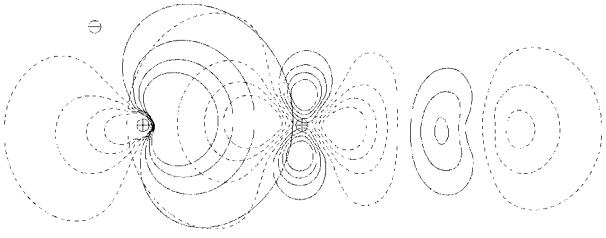

Figure 5. NBO contour plot illustrating the interaction between an electron lone pair of nitrogen with an antibonding Pd–Cl orbital in *R*,*R*-bis[(μ_2-hydrazine)$PdCl_2$].

To evaluate the role of the *trans* and *cis* influence, we carried out a second-order perturbation theory analysis of the Fock matrix with the NBO basis set. There are several charge transfers to be taken into account. These involve the charge transfer from the lone pair of nitrogen and a lone pair of halogen. In the former case the charge transfer takes place to an antibonding molecular orbital of the halogen atom *trans* to the nitrogen atom. The NBO delocalization energies were computed based on the deletion of off-diagonal elements between M–X bond orbitals and lone pairs of the nitrogen atom. There are some (mainly nickel) complexes, where there is a small but significant additional charge transfer to an antibonding molecular orbital of the halogen atom *cis* to the nitrogen atom. In the former case the related stabilization energy is defined as E_{trans}, and in the latter case E_{cis}. Furthermore, we shall use, for compari-

son purposes, an additional parameter, ΔE_{trans}, which is the difference between the stabilizing energies of the heterochiral and homochiral pairs. As for the charge transfers involving a lone pair of the halogen, there are two different antibonding orbitals that receive the charge, namely antibonding N–N and N–$H_{equatorial}$ molecular orbitals. In both cases the atoms involved are vicinal to the halogen atom. The related stabilizing energies are given as E_{XNN} and E_{XNH} [kcal/mol]. The values are shown in Table 6. Interestingly, there is no charge transfer from the coordinated electron lone pair to an antibonding M–N molecular orbital *trans* to the halogen atom.

Table 6. Selected results obtained from second-order perturbation theory analysis of the Fock matrix with the NBO basis set. The stabilizing energies are given in kcal/mol.

Fragment	Chirality	E_{trans}	ΔE_{trans}	E_{cis}	E_{XNN}	E_{XNH}
NiF_2	*RR*	74.59		2.91	5.97	0.29
NiF_2	*RS*	75.83	–1.24	2.91	3.46	1.77
$NiCl_2$	*RR*	67.66		3.02	5.70	0.38
$NiCl_2$	*RS*	68.11	–0.45	3.19	4.42	1.78
$NiBr_2$	*RR*	61.72		2.42	5.36	0.38
$NiBr_2$	*RS*	62.87	–1.15	2.65	4.25	1.71
NiI_2	*RR*	53.42		1.55	4.91	0.38
NiI_2	*RS*	53.08	–0.34	0.09	3.93	1.68
PdF_2	*RR*	71.65		0.07	5.42	0.18
PdF_2	*RS*	73.58	–1.92	0.08	3.00	1.36
$PdCl_2$	*RR*	61.15		0.00	4.66	0.19
$PdCl_2$	*RS*	62.14	–0.99	0.00	3.54	1.10
$PdBr_2$	*RR*	54.40		0.00	3.90	0.17
$PdBr_2$	*RS*	55.16	–0.76	0.00	3.13	0.97
PdI_2	*RR*	46.21		0.00	3.14	0.17
PdI_2	*RS*	46.82	–0.61	0.00	2.78	0.85
PtF_2	*RR*	96.48		0.00	3.88	0.18
PtF_2	*RS*	99.51	–3.03	0.00	2.29	1.22
$PtCl_2$	*RR*	88.93		0.00	4.50	0.17
$PtCl_2$	*RS*	91.09	–2.16	0.00	3.44	0.99
$PtBr_2$	*RR*	80.97		0.00	4.19	0.17
$PtBr_2$	*RS*	82.82	–1.85	0.00	3.37	0.90
PtI_2	*RR*	71.32		0.00	3.84	0.17
PtI_2	*RS*	73.04	–1.62	0.00	3.29	0.83

The results clearly show that there is always a charge transfer from a nitrogen lone pair to an antibonding M–X molecular orbital with a marked stabilization energy involved. Furthermore, the stabilization energy is always larger in the heterochiral complexes. There is also a correlation between the relative stabilization energies ΔE_{trans} and the relative total energies (E_{rel}), as shown in Figure 6. The r^2 value for the linear correlation is 0.854.

The E_{XNN} and E_{XNH} stabilization energies are clearly different in heterochiral and homochiral complexes. However, the effects are reversed so that the stabilizing energies E_{XNN} have larger values for homochiral complexes while the opposite holds true for the E_{XNH} values. Furthermore, the values tend to cancel out each other pairwise leaving E_{trans} to act as an explaining factor described in Figure 6.

The differences between the relative stabilization energies are obviously due to the different geometries caused by different orientations of the hydrazine molecules in the homo-

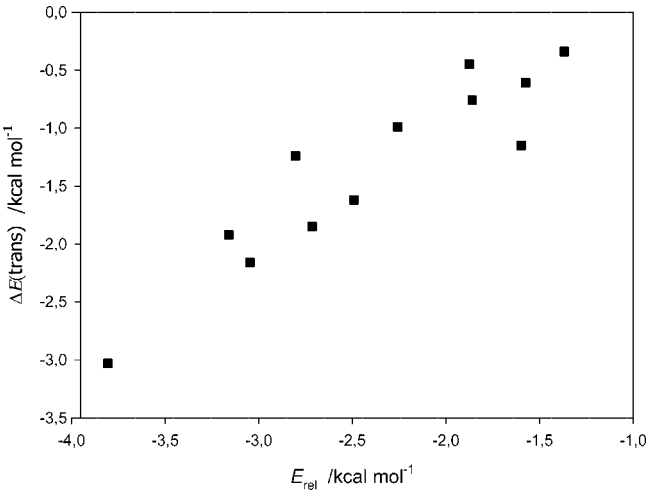

Figure 6. Scatter plot showing the correclation between the relative total energies E_{rel} and the relative stabilization energies indicating the *trans* influence.

and heterochiral complexes. This might also give a plausible explanation for the differences in the bond order and covalency of the M–N bonds. In the heterochiral complexes the values are higher, which might be explained by the smaller charge transfer into antibonding orbitals of the nitrogen atom. Furthermore, the different orientations also result in different L–M–L angles in the coordination spheres. In the heterochiral complexes the deviations are smaller leading to enhanced overlapping of the metal $d_{x^2-y^2}$-orbital and the electron lone pairs of the ligand atoms.

There is also a charge transfer from an electron lone pair of the nitrogen atom to another M–X antibonding molecular orbital. The stabilizing energies related to this *cis* influence are more than ten times smaller than the respective energies related to the *trans* influence in the nickel complexes. In the palladium and platinum complexes no *cis* influence was found, with the exception of the compounds composed of palladium and fluorine. Presumably, the *cis* influence might be correlated with the differences concerning the nickel complexes presented in Figure 3.

To conclude, we have shown that the electron lone pairs of the coordinated ligand atoms have a marked yet complicated role in bonding, and have not been properly considered in some important previous studies concerning bonding to platinum.[34]

Conclusions

Based upon the optimizations carried out at the B3LYP/LANL2DZ level of theory, the heterochiral complexes are more stable than the homochiral ones. The relative stability is correlated with the nature of both the metals and the anions. Moreover, the relative stability is correlated with the electronegativity values of the metals and the halogens. The QTAIM and NBO results indicated that the M–X bonds have marked ionic character with the halogen atoms show-

ing no hybridization. The coordinate M–X bonds are formed by an electron pair resting essentially on a p-type orbital of a halogen. Another profound difference is that the halogen atoms do not show any marked charge transfer to an antibonding M–N molecular orbital related to the *trans* influence. Instead, the contribution is seen in the composition of the electron lone pair of the nitrogen atom *trans* to the halogen atom. In sharp contrast to this, there is always a marked stabilization energy for the charge transition from the electron lone pair of nitrogen to an antibonding M–X orbital *trans* to the nitrogen atom. The M–N bonds formed formally by the electron lone pair of nitrogen also contain a contribution from the metal atom, thus indicating covalency of the bonds. The covalency, as well as the bond order, have a larger contribution in the M–N bonds of the heterochiral complexes. There is also a correlation between the relative distance of the bond critical points in the M–N bonds and the relative energy.

Although there are no experimental structures available, which could corroborate the calculated chiral discrimination, we feel confident that the predicted trends are correct.

Computational Methods

The geometries of the compounds were optimized by applying DFT methods and using Becke's three-parameter hybrid exchange functional in combination with the gradient-corrected correlation functional of Lee, Yang, and Parr.[35] The basis set applied in every calculation was LANL2DZ to include the relativistic effect.[36] The presence of true energy minima were checked by frequency calculations. No imaginary frequencies were found for the optimized structures. For every nickel complex it was necessary to check the stability of the wave function to see whether any instability existed from unrestricted contributions. We found instability in every case. After the check, the wave function was optimized to remove the contributions. The structures were then reoptimized using the optimized wave functions, their wave function stabilities rechecked, and frequencies recalculated. The calculations were carried out with the Gaussian 03 program suite.[37] The electronic properties were evaluated by QTAIM (Quantum Theory of Atoms in Molecules)[38] and NBO (Natural Bond Orbital) methods.[39] The NBO program used was the version installed in Gaussian 03. The QTAIM-based programs were MORPHY98,[40] AIMPAC,[41] and AIM2000.[42] We verified that similar geometries were obtained for some test cases using the Turbomole[43] program at the B3LYP/TZVP level of theory. Accordingly, the inclusion of polarization does not result in significant changes.

Supporting Information (see footnote on the first page of this article): Geometries of the optimized compounds and their respective energies.

Acknowledgments

This work was carried out with financial support from the Ministerio de Ciencia y Tecnología (Project No. BQU2003-01251). M. R. S. acknowledges the grant given by the Ministerio de Educación y Ciencia de España (SAB2003-0171). Thanks are given to the CTI (CSIC), CESGA, and CSC (Centre of Scientific Computing, Espoo, Finland) for the allocation of computer time.

[1] C. Girard, H. B. Kagan, *Angew. Chem. Int. Ed.* **1998**, *37*, 2922.
[2] I. Alkorta, J. Elguero, *J. Chem. Phys.* **2002**, *117*, 6463.
[3] K. Zborowski, I. Alkorta, J. Elguero, *J. Phys. Chem. A* **2006**, *110*, 7247.
[4] T. A. Beu, U. Buck, *Z. Phys. Chem.* **2000**, *214*, 437.
[5] G. Krainev, T. Shimizu, M. Ishigooka, K. Hiroya, M. Hatano, *Biochemistry* **1993**, *32*, 1951.
[6] I. Alkorta, O. Picazo, J. Elguero, *Tetrahedron Asym.* **2005**, *16*, 755.
[7] I. Alkorta, O. Picazo, J. Elguero, *J. Phys. Chem. A* **2005**, *109*, 9573.
[8] E. Housecroft, A. G. Sharpe, *Inorganic Chemistry*, 2nd ed., Pearson Education Limited, Harlow, **2005**, p. 686–687; B. J. Coe, S. J. Glenwright, *Coord. Chem. Rev.* **2000**, *203*, 5.
[9] M. Anderson, A. G. Orpen, *Chem. Commun.* **2001**, 2682–2683.
[10] K. Burdett, T. A. Albright, *Inorg. Chem.* **1979**, *18*, 2112.
[11] R. J. Deeth, *J. Chem. Soc., Dalton Trans.* **1993**, 781.
[12] P. D. Lyne, D. M. P. Mingos, *J. Organomet. Chem.* **1994**, *478*, 141.
[13] P. D. Lyne, D. M. P. Mingos, *J. Chem. Soc., Dalton Trans.* **1995**, 1635.
[14] N. Kaltsoyannis, P. Mountford, *J. Chem. Soc., Dalton Trans.* **1999**, 781.
[15] R. Salcedo, P. Sharma, A. Cabrera, S. Fomine, *J. Mol. Struct. (THEOCHEM)* **2002**, *579*, 151.
[16] C. Fave, M. Hissler, K. Sénéchal, I. Ledoux, J. Zyss, R. Réau, *Chem. Commun.* **2002**, 1674.
[17] H. Bent, *Chem. Rev.* **1961**, *61*, 275; J. P. Foster, F. Weinhold, *J. Am. Chem. Soc.* **1980**, *102*, 7211.
[18] C. R. Landis, T. K. Firman, D. M. Root, T. Cleveland, *J. Am. Chem. Soc.* **1998**, *120*, 1842.
[19] V. Jonas, C. Boehme, G. Frenking, *Inorg. Chem.* **1996**, *35*, 2097.
[20] M. Kaupp, *Chem. Eur. J.* **1999**, *5*, 3631; M. Kaupp, *Angew. Chem. Int. Ed.* **2001**, *40*, 3535.
[21] S. van Zutphen, E. Pantoja, R. Soriano, C. Soro, D. M. Tooke, A. L. Spek, H. den Dulk, J. Brouwer, J. Reedijk, *Dalton Trans.* **2006**, 1020.
[22] K. Yamamoto, S. Kawanishi, *J. Biol. Chem.* **1991**, *266*, 1509.
[23] K. Vimal, L. Jain, *Coord. Chem. Rev.* **2005**, *249*, 3075.
[24] J. Kozelka, E. Segal, C. Bois, *J. Inorg. Biochem.* **1992**, *47*, 67.
[25] S. Komeda, S. Bombard, S. Perrier, J. Reedijk, J. Kozelka, *J. Inorg. Biochem.* **2003**, *96*, 357.
[26] Y. Montet, J. Kozelka, *Inorg. Chim. Acta* **1999**, *284*, 103.
[27] O. Picazo, I. Alkorta, J. Elguero, M. R. Sundberg, *Inorg. Chem. Commun.* **2006**, *9*, 712.
[28] S. M. Free, J. W. Wilson, *J. Med. Chem.* **1964**, *7*, 395.
[29] L. Allred, *J. Inorg. Nuclear Chem.* **1961**, *17*, 215.
[30] a) R. F. W. Bader, *Atoms in Molecules: A Quantum Theory*, Oxford: Clarendon, **1990**; b) P. Popelier, *Atoms in Molecules – An Introduction*, Prentice Hall, Singapore, **2000**.
[31] a) P. Macchi, A. Sironi, *Coord. Chem. Rev.* **2003**, *238–239*, 383; b) C.-R. Lee, C.-C. Wang, K.-C. Chen, G.-H. Lee, Y. Wang, *J. Phys. Chem. A* **1999**, *103*, 156.
[32] C. Matta, J. Hernandez-Trujillo, *J. Phys. Chem. A* **2003**, *107*, 7496.
[33] R. Carlson, *Design and Optimization in Organic Synthesis*, Elsevier, Amsterdam, **1992**.
[34] H. Baik, R. A. Friesner, S. J. Lippard, *Inorg. Chem.* **2003**, *42*, 8615; D. V. Deubel, *J. Am. Chem. Soc.* **2002**, *124*, 5834.
[35] D. Becke, *J. Chem. Phys.* **1993**, *98*, 5648; C. Lee, W. Yang, R. G. Parr, *Phys. Rev. B* **1988**, *37*, 785.
[36] P. J. Hay, W. R. Wadt, *J. Chem. Phys.* **1985**, *82*, 299.
[37] M. J. Frisch, G. W. Trucks, H. B. Schlegel, G. E. Scuseria, M. A. Robb, J. R. Cheeseman, J. A. Montgomery Jr, T. Vreven, K. N. Kudin, J. C. Burant, J. M. Millam, S. S. Iyengar, J. Tomasi, V. Barone, B. Mennucci, M. Cossi, G. Scalmani, N. Rega, G. A. Petersson, H. Nakatsuji, M. Hada, M. Ehara, K. Toyota, R. Fukuda, J. Hasegawa, M. Ishida, T. Nakajima, Y. Honda, O. Kitao, H. Nakai, M. Klene, X. Li, J. E. Knox, H. P. Hratch-

ian, J. B. Cross, C. Adamo, J. Jaramillo, R. Gomperts, R. E. Stratmann, O. Yazyev, A. J. Austin, R. Cammi, C. Pomelli, J. W. Ochterski, P. Y. Ayala, K. Morokuma, G. A. Voth, P. Salvador, J. J. Dannenberg, V. G. Zakrzewski, S. Dapprich, A. D. Daniels, M. C. Strain, O. Farkas, D. K. Malick, A. D. Rabuck, K. Raghavachari, J. B. Foresman, J. V. Ortiz, Q. Cui, A. G. Baboul, S. Clifford, J. Cioslowski, B. B. Stefanov, G. Liu, A. Liashenko, P. Piskorz, I. Komaromi, R. L. Martin, D. J. Fox, T. Keith, M. A. Al-Laham, C. Y. Peng, A. Nanayakkara, M. Challacombe, P. M. W. Gill, B. Johnson, W. Chen, M. W. Wong, C. Gonzalez, J. A. Pople, *Gaussian 03*, Gaussian, Inc., Pittsburgh, PA, **2003**.

[38] a) R. F. W. Bader, *Atoms in Molecules: A Quantum Theory*, Clarendon, Oxford, **1990**; b) P. Popelier, *Atoms in Molecules – An Introduction*, Prentice Hall, Singapore, **2000**.

[39] a) E. Reed, L. A. Curtiss, F. Weinhold, *Chem. Rev.* **1988**, *88*, 899; b) F. Weinhold, C. Landis, *Valency and Bonding – A Natural Bond Orbital Donor-Acceptor Perspective*, Cambridge University Press, Cambridge, **2005**.

[40] *MORPHY98*, a program written by P. L. A. Popelier with a contribution from R. G. A. Bone, UMIST, Manchester, England, **1998**.

[41] F. W. Biegler-König, R. F. W. Bader, T. Ting-Hua, *J. Comput. Chem.* **1982**, *3*, 317.

[42] F. W. Biegler-König, J. Schönbom, *AIM2000 Version 2.0*, University of Applied Sciences, Bielefeld, Germany, **2002**.

[43] *The Program System TURBOMOLE, Version 5-5*: R. Ahlrichs, M. Bär, M. Häser, H. Horn, C. Kölmel, *Chem. Phys. Lett.* **1989**, *162*, 165.

Received: September 5, 2006
Published Online: November 17, 2006

